

Defect chemistry and oxygen diffusion in the $\text{HgBa}_2\text{Ca}_2\text{Cu}_3\text{O}_{8+\delta}$ superconductor: A computer simulation study

M. S. Islam* and L. J. Winch

Department of Chemistry, University of Surrey, Guildford, GU2 5XH, United Kingdom

(Received 22 May 1995)

Atomistic computer-simulation techniques are used to investigate the defect and ion transport properties of the Hg-based superconductors. We focus our attention on the highest- T_c material, $\text{HgBa}_2\text{Ca}_2\text{Cu}_3\text{O}_{8+\delta}$, for which we correctly reproduce the tetragonal structure using our potential model. Defect calculations predict the most favorable oxygen interstitial position as the O(4) $[\frac{1}{2}\frac{1}{2}0]$ site on the Hg plane, in agreement with diffraction studies. We find significant local relaxation around this defect. The complex defect, which involves substitution of Cu for Hg, is also examined in some detail. We calculate exothermic energies for the hole-doping (oxidation) reaction in which oxygen excess (δ) is incorporated as doubly charged O(4) interstitials and compensated by hole formation. Oxygen diffusion is attributed to interstitial migration, and is predicted to be both rapid and anisotropic.

I. INTRODUCTION

The discovery of superconductivity in $\text{HgBa}_2\text{CuO}_{4+\delta}$ with a T_c of 94 K (Ref. 1) has led to the synthesis of new Hg-based cuprate superconductors of the homologous series $\text{HgBa}_2\text{Ca}_{n-1}\text{Cu}_n\text{O}_{2n+\delta}$.²⁻⁵ The crystal structures are based upon rocksalt blocks $(\text{BaO})(\text{HgO}_8)(\text{BaO})$ alternating with anion-deficient perovskitelike blocks $(\text{CuO}_2)(\text{Ca}\square)(\text{CuO}_2)$. From this series, the three-layer compound $\text{HgBa}_2\text{Ca}_2\text{Cu}_3\text{O}_{8+\delta}$ (Hg-1223) was found to have a record T_c of 135 K (Refs. 2-5) or above 150 K under high pressure.^{6,7}

It is now clear that defect processes play a vital role in determining the properties of the superconducting oxides. For example, La_2CuO_4 shows high- T_c behavior when it is doped with Sr^{2+} , and the T_c of $\text{YBa}_2\text{Cu}_3\text{O}_{7-\delta}$ is strongly influenced by the extent of the oxygen deficiency (δ). For the Hg-based oxides, it is generally believed that excess oxygen atoms (as interstitial defects) are the primary doping mechanism to create the holes necessary for superconductivity. Diffraction experiments have already shown that the oxygen interstitials are present at the $[\frac{1}{2}\frac{1}{2}0]$ site in the center of the Hg plane.^{1,3,8-13} However, some studies have found an additional defect, which involves partial substitution of Hg by Cu coupled to the presence of oxygen in the $[\frac{1}{2}00]$ position between the Hg (Cu) atoms.^{8,12,13} More recently, single-crystal x-ray-diffraction results for $\text{HgBa}_2\text{CaCu}_2\text{O}_{6+\delta}$ suggest that the central interstitial is at an "off-center" position $[\frac{1}{2}0.40]$.¹²

Important questions, therefore, remain concerning the precise defect structure and the nature of the redox reaction responsible for the generation of the superconducting holes. In an attempt to gain further insight into these problems, we have investigated the three-layer Hg-1223 material using computer simulation techniques which are now well-established tools for probing solid-state properties at the atomic level. The present study extends previ-

ous simulation work on other high- T_c oxides, such as La_2CuO_4 (Refs. 14-16) and $\text{YBa}_2\text{Cu}_3\text{O}_7$ (Refs. 17-22), and will have general relevance to Hg-based superconductors.

II. SIMULATION METHODS

The atomistic simulations presented here use the same methods for the treatment of perfect and defective lattices as employed in previous studies of high- T_c oxides.¹⁴⁻²² The present account of these techniques (embodied in the CASCADE code²³) will be brief since comprehensive reviews are given elsewhere.^{24,25}

An important feature of these calculations is the treatment of lattice relaxation about the point defect or migrating ion. The Mott-Littleton approach is to partition the crystal lattice into two regions so that ions in a spherical inner region surrounding the defect are relaxed explicitly. In contrast, the remainder of the crystal, where the defect forces are relatively weak, is treated by more approximate quasicontinuum methods.

There is now ample evidence that given reliable interatomic potentials and a sufficiently large inner region these methods can produce accurate values of the energies of defect formation, migration, and substitution.^{24,25} The potentials describing the interatomic interactions are represented by ionic pairwise potentials of the form

$$\phi_{\alpha\beta}(r) = \frac{-Z_\alpha Z_\beta e^2}{r} + A_{\alpha\beta} \exp(-r/\rho_{\alpha\beta}) - C_{\alpha\beta}/r^6, \quad (1)$$

which includes the long-range Coulomb term and an analytical function to model overlap repulsions and van der Waals forces. Because charged defects will polarize other ions in the lattice, ionic polarizability must be incorporated into the potential model. The shell model²⁶ provides a simple description of such effects by treating each ion in terms of a core (representing the nuclear and core electrons) connected via a harmonic spring to a shell (representing the valence electrons). Despite the simple

TABLE I. Interatomic potentials.

(a) Short range			
Interaction	A (eV)	ρ (Å)	C (eV Å ⁶)
Hg ²⁺ . . . O ²⁻	648.5	0.3251	0.0
Ba ²⁺ . . . O ²⁻	2096.8	0.3522	8.0
Ba ²⁺ . . . Ba ²⁺	2663.7	0.3428	0.0
Ca ²⁺ . . . O ²⁻	1228.9	0.3372	0.0
Cu ²⁺ . . . O ²⁻	3860.6	0.2427	0.0
O ²⁻ . . . O ²⁻	22764.0	0.1490	43.0
(b) Shell model ^a			
Species	$Y(e)$	k (eV Å ⁻²)	
Hg ²⁺	1.50	598.0	
Ba ²⁺	1.848	29.1	
Ca ²⁺	1.26	34.0	
Cu ²⁺	1.00	99999	
O ²⁻	-2.389	3.88	

^a Y and k are the shell charge and harmonic force constant, respectively.

mechanical representation of the ionic dipole, shell-model potentials have proved to be effective in simulating the dielectric and lattice dynamical properties of ceramic oxides.

The short-range potential parameters assigned to each ion-ion interaction were derived by empirical fitting to observed structural properties. The mercury superconductors adopt tetragonal unit cells with $P4/mmm$ (No. 123) space group symmetry.^{1,8-11} For the first three members of the homologous series, namely, HgBa₂CuO_{4+δ} (Hg-1201), HgBa₂CaCu₂O_{6+δ} (Hg-1212), and HgBa₂Ca₂Cu₃O_{8+δ} (Hg-1223), the parameters were fitted simultaneously, resulting in a common set of interatomic potentials. This approach enables some information concerning the curvature of the energy surface to be included and has the added advantage of improved transferability. In the context of the Coulombic term, integral ionic charges are presumed, i.e., 2⁺ for Cu, 2⁺ for Hg, 2⁻ for O, etc., which enables a straightforward definition of hole states as Cu³⁺ or O⁻. Details of the

TABLE II. Lattice parameters and bond lengths (in Å) of Hg-1223.

Property	Calc.	Expt. ^a	$ \Delta $
Lattice parameter			
a	3.845	3.850	0.005
c	15.885	15.784	0.101
Bond lengths			
Hg-O(3)	1.953	1.950	0.003
Ba-O(2)	2.746	2.724	0.022
Ba-O(3)	2.866	2.851	0.015
Ca-O(1)	2.501	2.536	0.035
Ca-O(2)	2.448	2.450	0.002
Cu(1)-O(1)	1.929	1.925	0.004
Cu(2)-O(2)	1.923	1.925	0.002
Cu(2)-O(3)	2.849	2.810	0.039

^aChmaissem *et al.* (Ref. 11).

TABLE III. Calculated crystal properties of Hg-1223.

Property	Hg-1223
Lattice energy (eV)	-303.93
Elastic constants (10 ¹¹ dyn cm ⁻²)	
c_{11}	29.0
c_{12}	11.9
c_{13}	4.2
c_{33}	19.9
c_{44}	1.4
c_{66}	12.4
Dielectric constants	
$\langle \epsilon_0 \rangle$	10.18
$\langle \epsilon_\infty \rangle$	5.80

potentials and shell model parameters used in this study are given in Table I.

Prior to carrying out the defect calculations, energy minimization of the perfect lattice is performed to generate an equilibrium structure. The calculated and experimental bond distances and lattice parameters for the Hg-1223 system are listed in Table II. Examination of the differences shows good agreement between simulated and observed structures. The lattice energy, elastic, and dielectric constants for the perfect crystal have also been calculated and are reported in Table III. Unfortunately, corresponding experimental data are currently unavailable and would be useful for further validation and refinement of the potential model.

III. RESULTS AND DISCUSSION

A. Oxygen interstitial defect

As is the case with YBa₂Cu₃O_{6+δ} (YBCO), the charge carriers in Hg-1223 are formed not by aliovalent substitution, but by oxygen incorporation. Neutron-powder-diffraction experiments of Chmaissem *et al.*¹¹ found the doping mechanism to be the oxygen interstitial atoms at the $[\frac{1}{2} \frac{1}{2} 0]$ O(4) site, but found no evidence for additional defects. In contrast, recent x-ray-diffraction studies of Finger *et al.*¹² and neutron-diffraction studies of Wagner *et al.*¹³ suggest two distinct oxygen defect sites: (a) oxygen interstitial at the $[\frac{1}{2} \frac{1}{2} 0]$ O(4) site and (b) a complex defect comprised of oxygen at the $[\frac{1}{2} 0 0]$ O(5) site coupled to the substitution of Cu for Hg. Both defect sites are shown in Fig. 1. The oxygen occupancy of the O(4) site is found to vary systematically with T_c and is believed to be the variable doping defect for Hg-1223, whereas the occupancy of the O(5) site is essentially constant.¹³

To investigate this problem, calculations were first performed on the energies of isolated oxygen interstitials, which are given in Table IV. In all cases, the lattice ions surrounding the defect are allowed to relax in the energy minimization procedure. From examination of the interstitial energies, it is clear that it is relatively more favorable to form an isolated oxygen interstitial on the O(4) site located at the center of the Hg layer. This result is in accordance with neutron-diffraction studies of Hg-1223

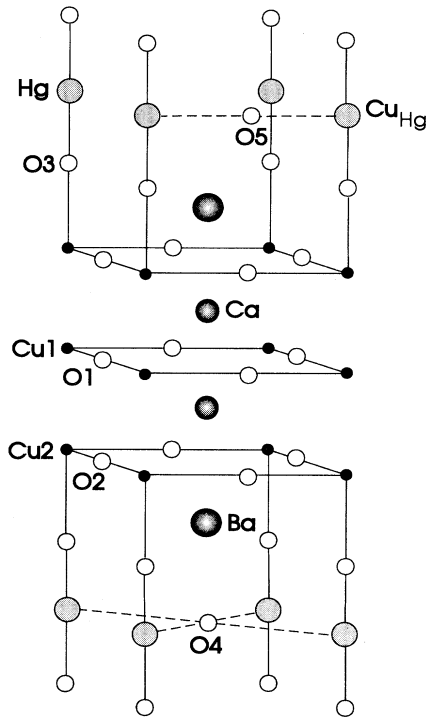


FIG. 1. Crystal structure of $\text{HgBa}_2\text{Ca}_2\text{Cu}_3\text{O}_{8+\delta}$ indicating the two possible defects that are partially occupied: (a) O(4) oxygen interstitial and (b) O(5) oxygen interstitial coupled with Cu on Hg.

by Chmaissem *et al.*¹¹ and Wagner *et al.*¹³ We should note that these “isolated” values are referenced to infinity and can be combined with other energy terms to derive Frenkel and redox energies.

As well as defect energetics, the simulations provide detailed information on the local relaxation around defect species. In particular, we find significant displacements of the nearest Hg and Ba ions of 0.6 and 0.1 Å, respectively, directly toward the O(4) interstitial. The relaxation of the Hg ions is illustrated in Fig. 2, indicating significant modification of the local structure.

Further to our investigation of the O(4) interstitial defect, we considered the antisite defect involving partial

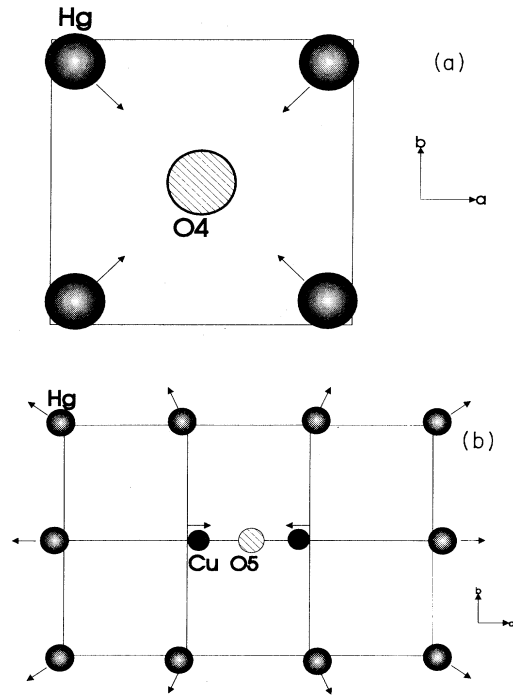


FIG. 2. Calculated ion relaxation around the two possible defects in the Hg plane: (a) O(4) oxygen interstitial. The Hg displacements are 0.58 Å. (b) O(5) oxygen interstitial coupled with Cu on Hg. The Cu displacements are 0.15 Å; the surrounding Hg ions have moved by less than 0.1 Å.

substitution of Cu^{2+} for Hg^{2+} coupled with the presence of oxygen on the $[\frac{1}{2} 0 0]$ O(5) site. Our simulation results reported in Table IV(b) suggest that, as an isolated defect, the Cu_{Hg} substitutional would be energetically unfavorable. Here we have examined whether the antisite defects could form from cation exchange:



The simulations result in a total reaction energy of 2.81 eV, which suggests that these defects would not favorably emerge from this process.

Calculations were then performed on defect complexes comprised of near-neighbor Cu_{Hg} substitutionals and O(5) oxygen interstitial atoms. Two cluster configurations were considered: first, a single Cu_{Hg} substitutional adjacent to O(5) and second, two Cu_{Hg} substitutionals neighboring O(5). The results are reported in Table IV(b), which gives the binding energies with respect to the component defects. The calculations reveal two main points. First, both the pair and trimer configurations are strongly bound, which suggests that the O(5) interstitial is stabilized by the substitution of Cu for Hg. Second, the binding energy and, hence, the degree of stabilization are slightly greater for the trimer complex comprised of two Cu atoms and a single O(5) interstitial. This would suggest a greater percentage population of Cu on Hg than the occupancy of the O(5) interstitial site. Again, we find significant local relaxation around these defect com-

TABLE IV. Calculated defect energies for Hg-1223.

(a) Isolated oxygen interstitials			
Interstitial site	E (eV) ^a		
O(4)[$\frac{1}{2} \frac{1}{2} 0$]	-20.98		
O(5)[$\frac{1}{2} 0 0$]	-20.20		
(b) Substitutional and complex defects			
Defect	E (eV) ^a	Binding energy (eV/Cu)	
Cu_{Hg} substitutional	1.37		
$[\text{Cu}_{\text{Hg}}\text{O}(5)]$	-20.34	-1.41	
$[2\text{Cu}_{\text{Hg}}\text{O}(5)]$	-20.44	-1.49	

^aZero reference at infinity.

TABLE V. Calculated hole energies (eV) in Hg-1223.

Defect	Hole energy	Electronic polarization energy
Cu ³⁺ (1)	3.29	6.22
Cu ³⁺ (2)	3.41	6.21
O ⁻ (1)	6.16	3.14
O ⁻ (2)	6.49	3.07
O ⁻ (3)	10.73	2.10

plexes; for example, the trimer [2Cu_{Hg}O(5)] is illustrated in Fig. 2, indicating near-neighbor Hg displacements of about 0.1 Å.

Recent thermogravimetric analysis (TGA) measurements have found that the occupancy of the [$\frac{1}{2}$ 00] O(5) site is essentially constant under oxidizing or reducing conditions and suggest that the O(5) oxygen is more strongly bound than oxygen atoms at O(4).¹³ Our calculated binding energies are consistent with this observation. In this context, it is interesting to note that the magnitude of the isolated Cu_{Hg} substitutional energy (1.37 eV) is comparable to the favorable binding energies to the O(5) interstitial (-1.4 eV). It is therefore possible that a subtle equilibrium exists between these two configurations which could be highly dependent upon the synthesis conditions and/or thermal history of the materials. This point may be relevant to why this defect is observed in some Hg-1223 samples^{12,13} but not in others.¹¹

B. Hole formation

Our approach to the investigation of electronic defects follows that first used for transition-metal oxides and subsequently the oxide superconductors.^{14,16,22} The positive holes are treated as Cu³⁺ and O⁻ polaron species; their calculated energies are reported in Table V together with the magnitude of the electronic polarization energy. Examination of the results indicates that the present calculations favor copper holes (Cu³⁺) over oxygen holes (O⁻). Although the hole energies for the two types of copper site in Hg-1223 are quite similar, the central plane with the square planar coordination [Cu(1)] has the most favorable energy. This results suggests a greater hole density in the Cu(1)-O plane, which is consistent with recent electronic structure calculations.²⁷ We acknowledge, however, that the question of whether such holes are predominantly in Cu(3d) or O(2p) bands remains controversial. It is almost certain that the hole state will have mixed Cu(3d)-O(2p) character. Our concern here is to understand how hole species might form; for this task, our simulation procedures have proved to be reliable. Ul-

timately, it will be necessary to employ quantum-mechanical methods to calculate the stability of hole states in these materials. The merit of our simulation approach is that it includes detailed estimates of lattice distortion and Coulomb energies which are difficult to make from other sources.

It is interesting to note that the polarization energies associated with the holes are substantial (6 eV) and indicate the strength of the electron-lattice interaction. Indeed, previous studies of La₂CuO₄ (Refs. 15 and 16) have shown that the interaction between the polarization fields could provide a hole-coupling mechanism to form "bipolarons." This is an obvious topic for further investigation.

In a similar fashion to YBa₂Cu₃O_{6+δ}, the charge carriers (holes) in HgBa₂Ca₂Cu₃O_{8+δ} are generated by incorporation of additional oxygen (δ), resulting in a degree of nonstoichiometry. In terms of defect chemistry, the oxygen "excess" is accommodated at interstitial sites with charge compensation by hole formation. This important oxidation reaction may be formulated as



where, in Kroger-Vink notation, O_i^{''} is a doubly charged oxygen interstitial and h' is a Cu³⁺ hole. Calculations in this area are amenable by our methods and are particularly useful in clarifying the mode of hole creation. We have already shown that the lowest-energy interstitial site is the O(4) position at the center of the Hg layer. The individual defect energies are then combined to give the energies of the oxidation reaction, which are reported in Table VI for the first three members of the Hg-based series.

Three main points emerge from these results. First, the negative values, indicating highly favorable reactions, clearly accord with observation as it is known that Hg-based materials readily oxidize with the uptake of the oxygen. Our results therefore confirm that this reaction is the primary hole-doping mechanism to generate p-type superconductivity in these oxides. Second, the calculated values are more exothermic than that in YBa₂Cu₃O_{6+δ} (Ref. 28) and agree well with a measured oxidation enthalpy of -136 kJ/mol (-1.41 eV) for Hg-1201 derived from recent oxygen annealing experiments.²⁹ Finally, the most favorable oxidation energy is found for the highest-T_c material Hg-1223, suggesting a wider level of oxygen excess (δ) in this system. It follows from the oxidation reaction (3) that the hole concentration will be related to the oxygen partial pressure (P_{O₂}) with a predicted dependence of + $\frac{1}{6}$.

In view of the debate concerning mixed valency and

TABLE VI. Energies of oxidation and charge disproportionation.

Process	Energies (eV)		
	HgBa ₂ CuO _{4+δ}	HgBa ₂ CaCu ₂ O _{6+δ}	HgBa ₂ Ca ₂ Cu ₃ O _{8+δ}
$\frac{1}{2}\text{O}_{2(g)} \rightarrow \text{O}_i'' + 2h'$	-1.47	-1.82	-2.25
$2\text{Cu}^{2+} \rightarrow \text{Cu}^+ + \text{Cu}^{3+}$	2.86	3.40	3.42

negative- U processes, it is also possible to obtain estimates of the charge-transfer reaction



The resulting energies, reported in Table VI, are large and positive and show that copper disproportionation is unfavorable; indeed, the magnitude is such that it is unlikely that this conventional negative- U process is of any significance in these materials.

C. Oxygen ion migration

Diffusion processes are known to be of considerable importance in influencing the properties of the cuprate superconductors. In particular, oxygen diffusion, which is relatively rapid in these materials, may affect the oxygen stoichiometry and hence the hole concentrations. Although there have been numerous reports on oxygen diffusion in YBCO materials,³⁰ there are currently no results on oxygen diffusion in the Hg-based oxides.

We have already obtained via simulation methods valuable energetic and mechanistic information on oxygen migration and lithium insertion in other high- T_c oxides^{17,19} which show good quantitative agreement with experiment. We have therefore examined possible migration mechanisms (interstitial and vacancy) in Hg-1223, mediated by conventional hopping between neighboring sites. The interstitial mechanism relates to the direct pathway between O(4) sites in the Hg plane. Since the formation energy of the O(1) vacancy in the Cu(1) plane is more favorable than either O(2) or O(3), we will only consider vacancy migration in the O(1) sublattice.

The migration energy is evaluated by calculating the defect energy of the mobile ion along the diffusion path with full lattice relaxation. In this way it is possible to map out an energy profile and to identify the saddle-point configuration. The resulting activation energies for Hg-1223 are reported in Table VII.

Examination of the results reveals that the O(4) interstitial mechanism emerges as the lowest-energy path with an activation energy of 0.68 eV. The corresponding energy profile is illustrated in Fig. 3. This result indicates that oxygen intercalation is facile in these materials and suggests their possible use as solid electrolytes or as oxygen sensors. As remarked earlier, there are at present limited oxygen transport data on Hg-based compounds with which direct comparisons may be made, although our calculated energy is consistent with observed values for other superconducting oxides.³⁰ We should note that, in contrast, previous simulation studies of oxygen migration predict vacancy mechanisms in both $\text{YBa}_2\text{Cu}_3\text{O}_{7-x}$ and $\text{YBa}_2\text{Cu}_4\text{O}_8$.¹⁷

TABLE VII. Calculated activation energies for oxygen ion migration in Hg-1223.

Mechanism	E_a (eV)
O(1)-O(1) vacancy	0.90
O(4)-O(4) interstitial	0.68

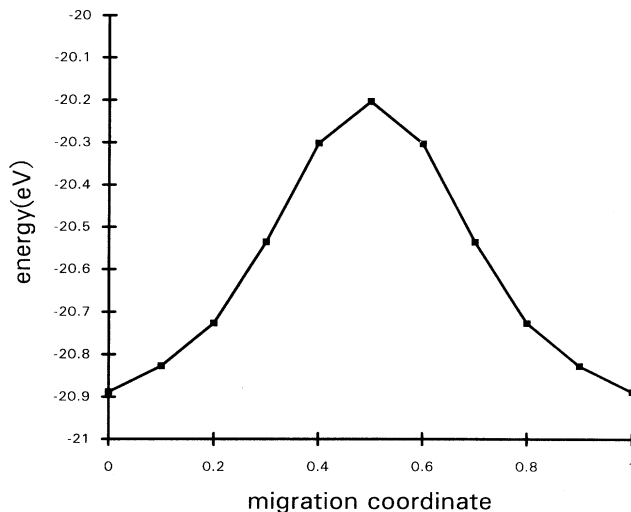


FIG. 3. Energy profile for interstitial migration between O(4) sites in Hg-1223.

In view of the favorable interstitial motion in the Hg layer, anisotropic ion transport is anticipated for single-crystal Hg-1223 with high diffusion coefficients (D_{ab}) in the ab plane. Indeed, such anisotropic transport behavior is a common feature in other cuprate superconductors.³⁰ Finally, it is worth noting that O(1) vacancy migration also has a relatively low-energy barrier, but will only become important when there is a significant concentration of oxygen vacancies.

IV. CONCLUSIONS

Atomistic computer simulations have yielded useful information on the defect chemistry and oxygen transport in the Hg-based oxides that are clearly relevant to their high- T_c behavior. Four main features emerge from the study.

(1) The most favorable oxygen interstitial energy is calculated for the O(4) $[\frac{1}{2}\frac{1}{2}0]$ position in accord with diffraction results. We find significant local relaxation about this defect, particularly displacement of Hg and Ba ions toward the O(4) site.

(2) The simulations of Hg-1223 support the additional defect cluster in which the O(5) $[\frac{1}{2}00]$ interstitial is coupled to the substitution of Cu for Hg. Our binding energies suggest that the O(5) chain oxygen is more strongly bound to the Cu than the O(4) oxygen; this may help to explain why the observed O(5) occupancy remains constant under different conditions. The calculated energies also suggest a subtle equilibrium for the $[\text{Cu}_{\text{Hg}}\text{O}(5)]$ defect that could be strongly dependent upon synthesis conditions; this may be relevant to why this defect is observed in some studies but not in others.

(3) We have examined the oxidation reaction [Eq. (3)] in which oxygen excess (δ) is incorporated as doubly charged O(4) interstitials and compensated by hole formation. The exothermic energies clearly support models in which this reaction is the major hole-doping mecha-

nism necessary for *p*-type superconductivity. We also find good agreement with the measured oxidation enthalpy for $\text{HgBa}_2\text{CuO}_{4+\delta}$.

(4) Oxygen diffusion is attributed to interstitial migration between O(4) sites in the Hg plane. We anticipate oxygen diffusion to be both rapid and anisotropic ($D_{ab} \gg D_c$) in these oxides.

ACKNOWLEDGMENTS

L.J.W. is supported by the EPSRC. The simulations were carried out on the supercomputer facilities at the University of London Computer Centre. We thank J. L. Wagner and J. D. Jorgensen for preprints of their work prior to publication.

*Author to whom correspondence should be addressed.

¹S. N. Putilin, E. V. Antipov, O. Chmaissem, and M. Marezio, *Nature* **362**, 226 (1993).

²A. Schilling, M. Cantoni, J. D. Gao, and H. R. Ott, *Nature* **363**, 56 (1993).

³E. V. Antipov, S. M. Loureiro, C. Chaillout, J. J. Capponi, P. Bordet, J. L. Tholence, S. N. Putilin, and M. Marezio, *Physica C* **215**, 1 (1993).

⁴M. Cantoni, A. Schilling, H. U. Nissen, and H. R. Ott, *Physica C* **215**, 11 (1993).

⁵Z. J. Huang, R. L. Meng, X. R. Qui, Y. Y. Sun, J. Kulik, Y. Y. Xue, and C. W. Chu, *Physica C* **217**, 1 (1993).

⁶C. W. Chu, L. Gao, F. Chen, Z. J. Huang, R. L. Meng, and Y. Y. Xue, *Nature* **365**, 323 (1993).

⁷M. Nunez-Regueiro, J. L. Tholence, E. V. Antipov, J. J. Capponi, and M. Marezio, *Science* **262**, 97 (1993).

⁸J. L. Wagner, P. G. Radaelli, D. G. Hinks, J. D. Jorgensen, J. F. Mitchell, B. Dabrowski, G. S. Knapp, and M. A. Beno, *Physica C* **210**, 447 (1993).

⁹O. Chmaissem, Q. Huang, S. N. Putilin, M. Marezio, and A. Santoro, *Physica C* **212**, 259 (1993).

¹⁰P. G. Radaelli, J. L. Wagner, B. A. Hunter, M. A. Beno, G. S. Knapp, J. D. Jorgensen, and D. G. Hinks, *Physica C* **216**, 29 (1993).

¹¹O. Chmaissem, Q. Huang, E. V. Antipov, S. N. Putilin, M. Marezio, S. M. Loureiro, J. J. Capponi, J. L. Tholence, and A. Santoro, *Physica C* **217**, 265 (1993).

¹²L. W. Finger, R. M. Hazen, R. T. Downs, R. L. Meng, and C. W. Chu, *Physica C* **226**, 216 (1994).

¹³J. L. Wagner, B. A. Hunter, D. G. Hinks, and J. D. Jorgensen,

Phys. Rev. B **51**, 15 407 (1995).

¹⁴M. S. Islam, M. Leslie, S. M. Tomlinson, and C. R. A. Catlow, *J. Phys. C* **21**, L109 (1988).

¹⁵C. R. A. Catlow, S. M. Tomlinson, M. S. Islam, and M. Leslie, *J. Phys. C* **21**, L1085 (1988).

¹⁶N. L. Allan and W. C. Mackrodt, *J. Am. Ceram. Soc.* **73**, 3175 (1990).

¹⁷M. S. Islam and R. C. Baetzold, *Phys. Rev. B* **40**, 10 926 (1989); *J. Mater. Chem.* **4**, 299 (1994).

¹⁸R. C. Baetzold, *Phys. Rev. B* **38**, 11 304 (1988); *Mol. Sim.* **12**, 77 (1994).

¹⁹M. S. Islam and C. Ananthamohan, *Phys. Rev. B* **44**, 9492 (1991); *J. Solid State Chem.* **100**, 371 (1992).

²⁰M. S. Islam, *Mol. Sim.* **12**, 101 (1994).

²¹X. Zhang, C. R. A. Catlow, S. C. Parker, and A. Wall, *J. Phys. Chem. Solids* **53**, 7761 (1993).

²²N. L. Allan and W. C. Mackrodt, *Mol. Sim.* **12**, 89 (1994).

²³M. Leslie (unpublished).

²⁴C. R. A. Catlow, *Annu. Rev. Mater. Sci.* **16**, 517 (1986).

²⁵A. M. Stoneham and J. H. Harding, *Annu. Rev. Phys. Chem.* **37**, 53 (1986).

²⁶B. G. Dick and A. W. Overhauser, *Phys. Rev.* **112**, 90 (1958).

²⁷R. P. Gupta and M. Gupta, *Physica C* **223**, 213 (1994).

²⁸M. E. Parks, A. Navrotsky, K. Mocala, E. Takayama-Muromachi, A. Jacobson, and P. K. Davies, *J. Solid State Chem.* **79**, 53 (1989).

²⁹Q. Xiong, Y. Y. Xue, F. Chen, Y. Cao, Y. Y. Sun, L. M. Liu, A. J. Jacobson, and C. W. Chu, *Physica C* **231**, 233 (1994).

³⁰A recent review is in J. L. Routbort and S. J. Rothman, *J. Appl. Phys.* **76**, 5615 (1994).

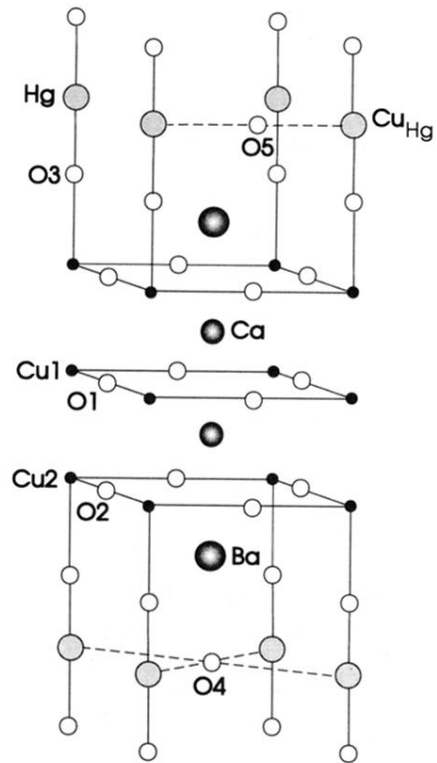


FIG. 1. Crystal structure of $\text{HgBa}_2\text{Ca}_2\text{Cu}_3\text{O}_{8+\delta}$ indicating the two possible defects that are partially occupied: (a) O(4) oxygen interstitial and (b) O(5) oxygen interstitial coupled with Cu on Hg.

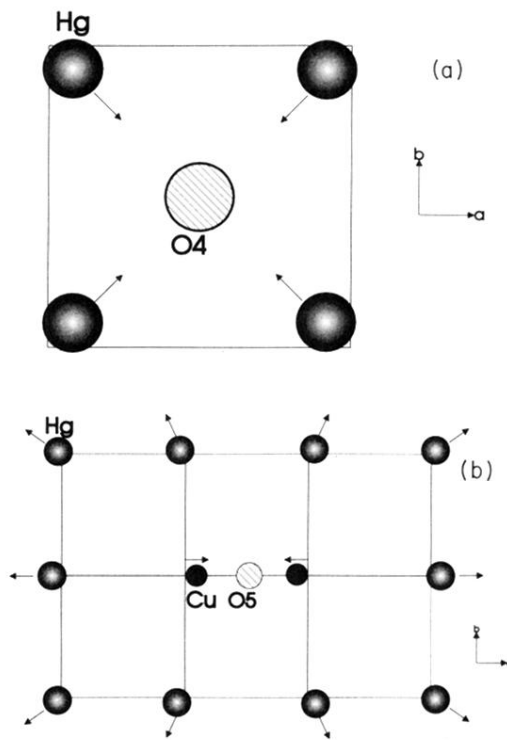


FIG. 2. Calculated ion relaxation around the two possible defects in the Hg plane: (a) O(4) oxygen interstitial. The Hg displacements are 0.58 Å. (b) O(5) oxygen interstitial coupled with Cu on Hg. The Cu displacements are 0.15 Å; the surrounding Hg ions have moved by less than 0.1 Å.